Research Article | Vol. 26, No. 8 | 16 Apr 2018 | OPTICS EXPRESS 10519
Optics EXPRESS

Real-time 100 Gbps/λ/core NRZ and EDB IM/DD transmission over multicore fiber for intra-datacenter communication networks

Rui Lin,[1,2,8] Joris Van Kerrebrouck,[3,8] Xiaodan Pang,[2,4] Michiel Verplaetse,[3] Oskars Ozolins,[4] Aleksejs Udalcovs,[4] Lu Zhang,[2,5] Lin Gan,[1] Ming Tang,[1] Songnian Fu,[1] Richard Schatz,[2] Urban Westergren,[2] Sergei Popov,[2] Deming Liu,[1] Weijun Tong,[6] Timothy De Keulenaer,[7] Guy Torfs,[3] Johan Bauwelinck,[3] Xin Yin,[3] and Jiajia Chen[2,*]

[1]*Huazhong University of Science and Technology, Wuhan, China*
[2]*KTH Royal Institute of Technology, Electrum 229, Kista, Sweden*
[3]*Department of Information Technology (INTEC) – IDLab, Ghent University –imec, Belgium*
[4]*Networking and Transmission Laboratory, RISE Acreo AB, Kista, Sweden*
[5]*Shanghai Jiao Tong University, Shanghai, China*
[6]*Yangtze Optical fiber and Cable Joint Stock Limited Company (YOFC), Wuhan, China*
[7]*BiFAST, spin-off of IDLab, Ghent University–imec, Ghent, Belgium*
[8]*Rui Lin and Joris Van Kerrebrouck contributed equally to this work*
[*]*jiajiac@kth.se*

Abstract: A BiCMOS chip-based real-time intensity modulation/direct detection spatial division multiplexing system is experimentally demonstrated for both optical interconnects. 100 Gbps/λ/core electrical duobinary (EDB) transmission over 1 km 7-core multicore fiber (MCF) is carried out, achieving KP4 forward error correction (FEC) limit (BER < 2E-4). Using optical dispersion compensation, 7 × 100 Gbps/λ/core transmission of both non-return-to-zero (NRZ) and EDB signals over 10 km MCF transmission is achieved with BER lower than 7% overhead hard-decision FEC limit (BER < 3.8E-3). The integrated low complexity transceiver IC and analog signal processing approach make such a system highly attractive for the high-speed intra-datacenter interconnects.

OCIS codes: (060.2330) Fiber optics communications; (060.2360) Fiber optics links and subsystems; (060.4510) Optical communications.

References and links

1. Cisco, "Cisco global cloud index 2015-2020," 2016.
2. C. Xie, "Scalability of optical technologies for growing exascale datacenters," in Workshop in ECOC, 2017.
3. K. Schmidtke, "Increasing datacenter bandwidth: a network or a technology issue?" in Workshop in ECOC, 2017.
4. "China Telecom- inner Mongolia information park." [Online]. Available: http://worldstopdatacenters.com/china-telecom-inner-mongolia-information-park/.
5. L. F. Suhr, J. J. Vegas Olmos, B. Mao, X. Xu, G. N. Liu, and I. T. Monroy, "112-Gbit/s x 4-lane duobinary-4-PAM for 400GBase," in 2014 The European Conference on Optical Communication (ECOC), 2014.
6. M. I. Olmedo, T. Zuo, J. B. Jensen, Q. Zhong, X. Xu, S. Popov, and I. T. Monroy, "Multiband carrierless amplitude phase modulation for high capacity optical data links," J. Lightwave Technol. **32**(4), 798–804 (2014).
7. M. I. Olmedo, Z. Tianjian, J. B. Jensen, Z. Qiwen, X. Xu, and I. T. Monroy, "Towards 400GBASE 4-lane Solution using direct detection of multiCAP signal in 14 GHz bandwidth per lane," PDP in *OFC*, (2013).
8. C. Kottke, C. Caspar, V. Jungnickel, R. Freund, M. Agustin, and N. Ledentsov, "High speed 160 Gb/s DMT VCSEL transmission using pre-equalization," in *OFC* (2017).
9. H. Chien, Z. Jia, J. Yu, and F. Li, "160-Gbps/λ IMDD optical links based on Nyquist 256QAM," in *OFC (*2016).
10. J. Lee, "Demonstration of 112-Gbit/s optical transmission using 56GBaud PAM-4 driver and clock-and-data recovery ICs," in *ECOC* (2015).

#320872 https://doi.org/10.1364/OE.26.010519
Journal © 2018 Received 30 Jan 2018; revised 27 Mar 2018; accepted 29 Mar 2018; published 11 Apr 2018

Optics EXPRESS

11. J. Verbist, J. Lambrecht, M. Verplaetse, J. Van Kerrebrouck, and S. A. Srinivasan, "DAC-less and DSP-free PAM-4 transmitter at 112 Gb/s with two parallel GeSi electro-absorption modulators," PDP, ECOC **2**(3), 33–35 (2017).
12. Socionext Inc., "World's lowest-power IC for single-wavelength, 100Gbps transmission over SMF optical links," 2016.
13. J. Verbist, M. Verplaetse, S. A. Srinivasan, P. De Heyn, T. De Keulenaer, R. Vaernewyck, R. Pierco, A. Vyncke, P. Verheyen, S. Balakrishnan, G. Lepage, M. Pantouvaki, P. Absil, X. Yin, G. Roelkens, G. Torfs, J. Van Campenhout, and J. Bauwelinck, "Real-time 100 Gb / s NRZ-OOK transmission with a silicon photonics GeSi electro-absorption modulator," in *IEEE Optical Interconnects Conference (OI)*, (2017).
14. X. Yin, M. Verplaetse, R. Lin, J. V. Kerrebrouck, O. Ozolins, T. D. Keulenaer, X. Pang, R. Pierco, R. Vaernewyck, A. Vyncke, R. Schatz, U. Westergren, G. Jacobsen, S. Popov, J. Chen, G. Tofs, and J. Bauwelinck, "First demonstration of real-time 100 Gbit/s 3-level duobinary transmission for optical interconnects," in PDP, *ECOC*, 2016.
15. R. G. H. van Uden, R. A. Correa, E. A. Lopez, F. M. Huijskens, C. Xia, G. Li, A. Schülzgen, H. de Waardt, A. M. J. Koonen, and C. M. Okonkwo, "Ultra-high-density spatial division multiplexing with a few-mode multicore fibre," Nat. Photonics **8**(11), 865–870 (2014).
16. D. J. Richardson, J. M. Fini, and L. E. Nelson, "Space-division multiplexing in optical fibres," Nat. Photonics **7**(5), 354–362 (2013).
17. A. Li, X. Chen, A. Al Amin, J. Ye, and W. Shieh, "Space-division multiplexed high-speed superchannel transmission over few-mode fiber," J. Lightwave Technol. **30**(24), 3953–3964 (2012).
18. N. Bai, C. Xia, and G. Li, "Adaptive frequency-domain equalization for the transmission of the fundamental mode in a few-mode fiber," Opt. Express **20**(21), 24010–24017 (2012).
19. Z. Feng, H. Ji, M. Tang, L. Yi, L. Gan, L. Xue, Q. Wu, B. Li, J. Zhao, W. Tong, S. Fu, D. Liu, and W. Hu, "C-band real-time 400/300 Gb/s OOK bidirectional interconnection over 20 km multicore fibers," Chin. Opt. Lett. **15**(8), 12–16 (2017).
20. R. Lin, X. Pang, J. Van Kerrebrouck, M. Verplaetse, O. Ozolins, A. Udalcovs, L. Zhang, L. Gan, M. Tang, S. Fu, R. Schatz, U. Westergren, S. Popov, D. Liu, W. Tong, T. De Keulenaer, G. Torfs, J. Bauwelinck, X. Yin, and J. Chen, "Real-time 100 Gbps/λ/core NRZ and EDB IM/DD transmission over 10 km multicore fiber," in *OFC*, 2018.
21. T. De Keulenaer, G. Torfs, Y. Ban, R. Pierco, R. Vaernewyck, A. Vyncke, Z. Li, J. H. Sinsky, B. Kozicki, X. Yin, and J. Bauwelinck, "84 Gbit/s SiGe BiCMOS duobinary serial data link including serialiser/deserialiser (SERDES) and 5-tap FFE," Electron. Lett. **51**(4), 343–345 (2015).
22. M. Yoneyama, K. Yonenaga, Y. Kisaka, and Y. Miyamoto, "Differential precoder IC modules for 20-and 40-Gbit/s optical duobinary transmission systems," IEEE Trans. Microw. Theory Techn. **47**(12), 2263 (1999).
23. O. Ozolins, M. I. Olmedo, X. Pang, S. Gaiarin, A. Kakkar, A. Udalcovs, K. M. Engenhardt, T. Asyngier, R. Schatz, J. Li, F. Nordwall, U. Westergren, D. Zibar, S. Popov, and G. Jacobsen, "100 GHz EML for high speed optical interconnect applications," in *ECOC*, 2016.
24. M. Chaciński, U. Westergren, R. Schatz, B. Stoltz, S. Hammerfeldt, and L. Thylén, "Monolithically integrated 100 GHz DFB-TWEAM," J. Lightwave Technol. **27**(16), 3410–3415 (2009).
25. M. Verplaetse, R. Lin, J. Van Kerrebrouck, O. Ozolins, T. De Keulenaer, X. Pang, R. Pierco, R. Vaernewyck, A. Vyncke, R. Schatz, U. Westergren, G. Jacobsen, S. Popov, J. Chen, G. Torfs, J. Bauwelinck, and X. Yin, "Real-time 100 Gb/s transmission using three-level electrical duobinary modulation for short-reach optical interconnects," J. Lightwave Technol. **35**(7), 1313–1319 (2017).
26. Z. Feng, L. Xu, Q. Wu, M. Tang, S. Fu, W. Tong, P. P. Shum, and D. Liu, "Ultra-high capacity WDM-SDM optical access network with self-homodyne detection downstream and 32QAM-FBMC upstream," Opt. Express **25**(6), 5951–5961 (2017).
27. M. Becker, A. Lorenz, T. Elsmann, I. Latka, A. Schwuchow, S. Dochow, R. Spittel, J. Kobelke, J. Bierlich, K. Schuster, M. Rothhardt, and H. Bartelt, "Single-mode multicore fibers with integrated bragg filters," J. Lightwave Technol. **34**(19), 4572–4578 (2016).

1. Introduction

Emerging mobile and cloud applications drive ever-increasing capacity demands in datacenters, which are expected to handle 99% of the global network data by 2020 [1]. In the near future, the need for 400G connectivity and beyond has been crystal clear for intra-datacenter networks [2, 3]. Intra-datacenter interconnects (DCIs) comprise server-to-ToR (top of rack), ToR-to-fabric, and inter-fabric links, covering links with transmission distances from tens of meters to several kilometers [4].To address the growing capacity demands in DCIs, research efforts have been put on improving the single lane rate, e.g., to 100 Gbps and beyond with intensity modulation and direct detection (IM/DD) systems [5–9]. In addition, low latency should be guaranteed for time-critical services involving DCNs (e.g., remote control), and therefore heavy digital signal processing (DSP) needs to be avoided. Recent demonstrations over 100 Gbps real-time IM/DD systems were reported using advanced

Optics EXPRESS

modulation formats, e.g. four-level pulse amplitude modulation (PAM-4) [10, 11] and discrete multitone (DMT) [12]. Nevertheless, advancements in low power consumption and low complexity transceiver integrated circuit (IC) designs make simple non-return-to-zero (NRZ) [13] and partial response modulation format, such as electrical duo-binary (EDB) [14], attractive for high-speed real-time communications in optical interconnects, especially when communications are achievable with simple analog equalization.

Meanwhile, apart from the improvements of the lane rate, scaling up the lane count per fiber is being intensively investigated. Transporting data using the spatial division multiplexing (SDM) approach, for instance, through different modes in a single fiber, i.e., few mode fibers (FMFs) or in independent cores of multicore fibers (MCFs) are widely studied in [15–17]. FMF based short reach interconnects [18] suffer from the differential mode dispersion and modal interference which needs to be addressed with complex DSP and therefore may hinder its deployment in the DCIs. In short reach communication systems, where transceiver complexity and energy consumption are among the main concerns, MCF-based SDM system is appreciated for its high capacity as well as good performance.

Recently, a real-time multicore fiber (MCF)-based IM/DD system was reported in [19] where the lane rate (i.e., the data rate per wavelength per core) is limited to 25 Gbps. In this paper, using an in-house developed BiCMOS based transmitter and receiver chipset, MCF and fan-in/fan-out (FI/FO) devices, we experimentally demonstrate a real-time IM/DD transmission system using 100 Gbps/λ/core NRZ and EDB modulation formats over a 7-core fiber, which significantly advances the state-of-the-art lane rate while verifying its potential to scale up the lane count per fiber. EDB signaling over 1 km 7-core fiber is demonstrated, achieving KP4 FEC limit with bit error rate (BER) = 2E-4. Employing optical dispersion compensation, the 7% overhead (OH) hard decision (HD) FEC limit (i.e., BER = 3.8E-3) and KP4 FEC limit can be achieved for NRZ and EDB signals, respectively, after 10 km transmission. As an extension of our previous work in [20], this paper includes the following two new contributions: (i) we elaborate the in-house designed electrical and optical components for the experiment setup, including the electrical transceivers, the broadband optical transmitter, the MCF and the fan-in/fan-out (FI/FO); and (ii) the experiment results are extensively extended by including the link property and performance of NRZ/EDB signaling over 1 km.

The remainder of this paper is organized as follows: Section 2 presents the components used in the link. Section 3 and 4 discuss the experiment setup and results of the real-time transmission over 1 km and 10 km MCF at 100 Gbps/λ/core. Conclusions and future work are drawn in Section 5.

2. In-house developed components for MCF enabled high-speed optical interconnects

2.1 Electrical transceiver

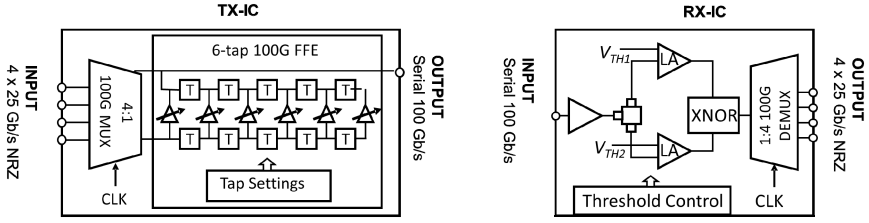

Fig. 1. Schematic diagram of the transceiver architecture used in the experiment.

A schematic diagram of the electrical transceiver is shown in Fig. 1. Both the transmitter (Tx) and the receiver (Rx) are designed in-house by the BiFAST team in a 0.13 µm BiCMOS technology, occupying 1555µm × 4567 µm and 1926 µm × 2585 µm respectively. The 4-to-1

Optics EXPRESS

MUX in the TX IC is capable of multiplexing 4 lanes of 25 Gbps signals into a serial 100 Gbps stream. A six-tap analog feedforward equalizer (FFE) is designed as a tapped delay line, where each gain cell can be independently tuned with a precision of 8 bit. The FFE shapes the NRZ input waveform together with the subsequent components in the link. At the receiver side, the RX IC [21] consists of 2 parallel level-shifting limiting amplifiers (LA), an XOR-gate and a 1-to-4 DEMUX. The NRZ detection needs only one LA to be configured and kept constant. For EDB transmission, 4 lanes of 25 Gbps should be precoded by a flip-flop and an XOR-gate operation [22] and then fed into the 4-to-1 MUX. At the receiver side, the threshold of both LAs need to be controlled to ensure the upper and lower eye of the EDB signals can be correctly extracted from the varied received optical power. An XOR gate architecture is needed at the receiver to decode the EDB signals. The energy consumption of the TX and RX are less than 1 W and 1.2 W respectively [14].

2.2 Electro-absorption modulated laser

The monolithically integrated distributed feedback laser with traveling-wave electro-absorption modulator (DFB-TWEAM) [23] was in-house fabricated, grown by metal organic vapor phase epitaxy (MOVPE) on n-doped InP substrate [24]. The gain section of the laser consists of 7 quantum wells (QWs), each of which is 7 nm thick, whereas the modulator has 12 QWs with a thickness of 9 nm. The laser and the modulator are integrated using a butt-joint technique. The 3 dB bandwidth of the DFB-EAM is beyond 90 GHz. The P(I) and P(V) characteristics of the transmitter operating at room temperature (22 °C) can be found in [25]. The DFB-laser exhibits a threshold of 25 mA and an output slope of 0.4 W/A. In the experiment, the DFB is biased at 117.0 mA with a output power of ~3 mW. the EAM is biased at −1.85 V and a 50 GHz RF amplifier is used to drive the DFB-TWEAM [6] with the swing around 2.2 Vpp.

2.3 7-core MCF and FI/FO

The cross section of the 7-core fiber and the compact low-loss FI/FO modules are shown in the insets in Fig. 2. Cores of the trench-assisted MCF are designed as a hexagonal distribution. The cladding diameter of the MCF is 150 μm and the core pitch is set as 42 μm. Comparable properties can be found in each core of the fabricated MCF and single mode fiber (SMF) in terms of attenuation, dispersion and mode field diameter [26]. The crosstalk between adjacent cores is as low as −45 dB/100 km. The average attenuation per core is less than 0.2 dB/km at 1550 nm. The FI/FO is realized by chemically etching the 7 bare SMF until the cladding diameter matches the MCF core pitch and arranging them in the hexagonal lattice [7]. The insertion loss per FI/FO is less than 1.5 dB. The end-to-end insertion loss of each core including MCF as well as a pair of FI/FO modules is listed in Table 1, where the difference is mainly caused by the fabrication of the FI/FO modules and the coupling of the fiber.

Table 1. End-to-end insertion loss including MCF and FI/FO modules

Core No.	End-to-end insertion loss of 1 km MCF	End-to-end insertion loss 10 km MCF
Core 1	2 dB	3.9 dB
Core 2	5.3 dB	6.6 dB
Core 3	3.3 dB	6.4 dB
Core 4	5.2 dB	5.2 dB
Core 5	4.2 dB	8.1 dB
Core 6	2.3 dB	5.7 dB
Core 7	5.0 dB	6.9 dB

Optics EXPRESS

3. Experiment setup

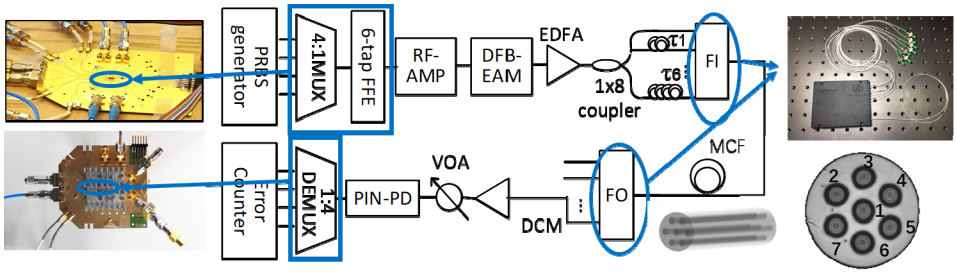

Fig. 2. Experiment setup.

The experiment setup is illustrated in Fig. 2. A Xilinx Virtex Ultrascale FPGA generates four electrical 2^7-1 pseudo-random bit streams (PRBS) at 25 Gbps, which are shifted with a delay of 0, 32, 64 and 96 bits and multiplexed into a 100 Gbps NRZ signal by the TX IC. The 6-tap FFE at the TX side is used to compensate the frequency roll-off and dispersion induced inter-symbol-interference in the link. A 50 GHz RF amplifier is used to drive the DFB-TWEAM [6] with the swing around 2.2 Vpp. The DFB-laser and the EAM are biased at 117.0 mA and −1.85 V, respectively. The output signal centered at 1548.7 nm, is firstly amplified by an erbium-doped fiber amplifier (EDFA) and then divided into 8 branches using a 1x8 power splitter. Seven streams of the split signals (1 splitter output is not used) are further de-correlated with different delays, and launched into the 7 cores of the MCF via the low-loss and low crosstalk FI/FO module split and connected to seven individual SMF pigtails at the other end. After the MCF transmission, the spatial channels are demultiplexed by another FI/FO module so that the signals in each core can be connected to a SMF. A variable optical attenuator (VOA) is employed to adjust the received optical power before the pre-amplifier and an InP-based PIN-PD (>90 GHz 3-dB BW) with a responsivity of 0.2 A/W. The received 100 Gbps data is deserialized by the RX IC into 4 × 25 Gbps streams for real-time error detection. In our experimental setup, the EDFA at the transmitter side is used to compensate the splitting loss of the optical coupler while the one at the receiver side is used to adjust the received optical power to measure the BER performance. These EDFAs can be avoided in the practical implementations.

Comparing to the EDB, the NRZ detection, as mentioned previously, needs only one LA to be configured which can be kept constant regardless of the power fluctuation, and therefore has potentially lower RX complexity. The initial tap weights in the FFE for the NRZ or EDB are calculated by using a least square error algorithm to fit the linear combination of the impulse responses to an ideal pulse, as shown in Fig. 3(a) and 3(b). Once the taps are set, the system can operate continuously without changing the filter configuration. In the measurements, the tap weights are further adapted to minimize the BER. For the 10 km MCF transmission, a fixed dispersion compensation module (DCM) of −159 ps/nm is used for coarse dispersion compensation. The dispersion compensation can be realized by writing gratings in multicore fibers, so that DCM is not necessary for each core [27].

Optics EXPRESS

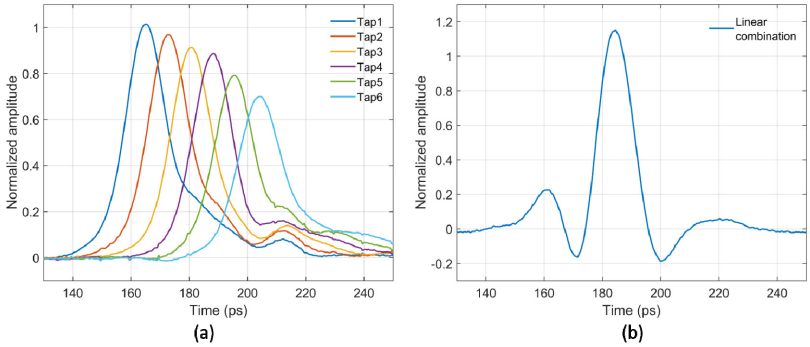

Fig. 3. (a) Impulse responses of each tap in the FFE, (b) linear combination with the optimum tap weights.

4. Results and discussion

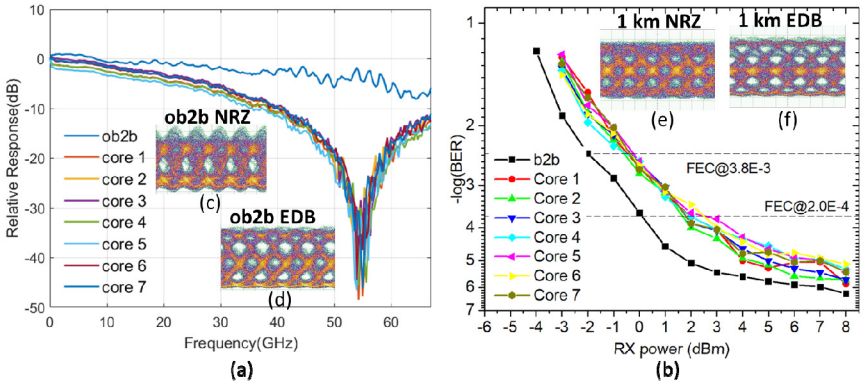

Fig. 4. (a) Relative frequency response of the b2b optical link and different cores of 1 km MCF, (b) BER of real-time 100 Gbps EDB signal measurement for b2b and different cores after 1 km MCF transmission, eye diagrams of b2b (c) NRZ signal and (d) EDB signal measured for optical b2b, eye diagram of (e) NRZ signal and (f) EDB signals measured at core 7 after 1 km MCF transmission.

4.1 NRZ and EDB transmission over 1 km MCF

Figure 4 shows the end-to-end relative frequency responses of the optical back-to-back (b2b) and after transmissions over all the 7 cores of the 1 km MCF. Each curve is normalized with respect to his own direct current response. Only small variations among the cores are observed, which can attribute to the imperfect fabrication of the fiber cores. A dispersion-induced RF fading notch appears at around 55 GHz for all the cores. The eye diagrams of the received NRZ and EDB signals in the optical b2b configuration are widely open (see Fig. 4(c) and 4(d), respectively) thanks to the broadband DFB-EAM and the PIN-PD, as well as the equalization at the transmitter. The end-to-end bandwidth of the link is mainly limited by the fiber chromatic dispersion. After transmission, the middle eye of the NRZ stream is hardly open, as shown in Fig. 4(e). With a received power of ~6 dBm, the best BER that the detected NRZ signal reaches is 4.0E−3. On the other hand, 100 Gbps EDB signal suffers less from the chromatic distortion because of the required bandwidth is only half of that for NRZ signal, as previously shown in [23]. BER performance of the received EDB signal and the eye-diagram received at core 7 after 1 km MCF transmission can be seen in Fig. 4(b) and 4(f). Reaching

Optics EXPRESS

7%-OH HD-FEC limit, the sensitivity of b2b configuration is –2dBm. The power penalty due to the 1 km MCF transmission is around 1.7 dB.

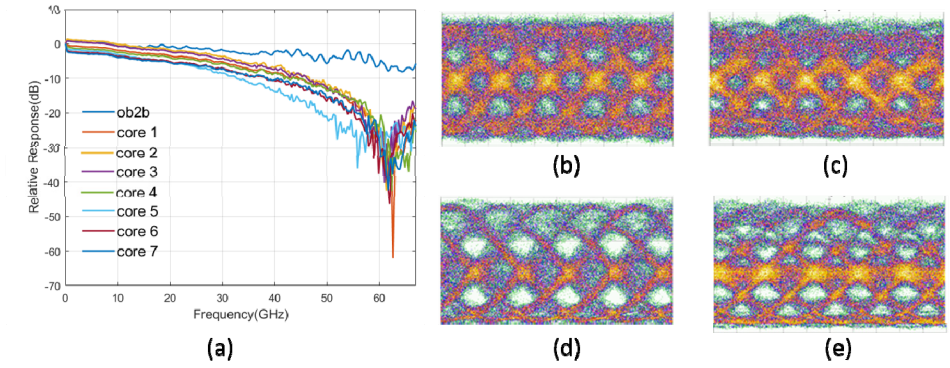

Fig. 5. Relative frequency response of the b2b optical link and different cores of 10 km MCF, eye diagrams of the NRZ signal measured at core 4 (b) and core 5 (c), EDB signal measured at core 4 (d) and core 5 (e) with the received power of 6 dBm.

4.2 NRZ and EDB transmission over 10 km MCF

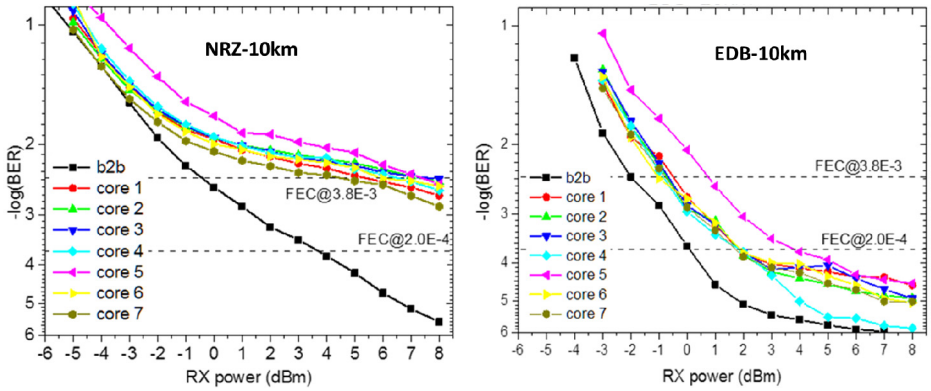

Fig. 6. BER of the real-time 100Gbps (a) NRZ signals and (b) EDB signals measured for b2b transmission and different cores after 10 km MCF.

The relative channel responses over the optical b2b and all the cores of the 10 km MCF are shown in Fig. 5. One can observe a frequency dip at around 62 GHz across all the cores, indicating that a residual dispersion of 16 ps/nm is not fully compensated by the DCM. The variation among different cores is caused by insertion loss and end face reflection of the fabricated FI/FO devices. The eye-diagrams of the received signals after 10 km MCF transmission in core 4 and core 5 are shown in Fig. 5(b) and 5(e) with the received optical power of ~6 dBm. Inter-symbol-interference due to fiber transmission is the main contributor to the eye closing comparing to the b2b case. We evaluate the optical transmission performance of both the NRZ and the EDB at 100 Gbps using the experiment setup shown in Fig. 2. Apart from the fixed DCM, the six-tap analog FFE at the TX is adjusted to enhance the system tolerance towards the imperfect dispersion compensation. The BER curves of the received optical signals after 10 km MCF transmission using the NRZ and the EDB are shown in Fig. 6, respectively. For the NRZ case, BER = 2.8E−6 is reached and no error floor is observed in b2b configuration thanks to the broadband optical transceiver. In the 10 km MCF transmission cases, the signal quality is degraded due to the chromatic dispersion. The transmission in all the cores saturates at BER around 3E-3, yet below the 7%-OH HD-FEC. The power penalties compared with the b2b transmission of NRZ signal ranges from 4.4 dB

Optics EXPRESS

to 7.3 dB in different cores with an average value of 6.3 dB. In the EDB transmission, except for core 5, all the other spatial channels have similar receiver sensitivities to reach BER of 3.8E−3 after the 10 km MCF transmission. The sensitivity variation is mainly due to the imperfect fabrication consistency of each core and the end face reflection in the MCF link including FI/FO. The EDB requires only half bandwidth comparing to NRZ, as a result, less filtering effect over the link causes much lower penalty (<2 dB) compared to the b2b configuration. The eye diagrams of the received EDB signals with the best (core 4) and the worst (core 5) transmission performances are shown in Fig. 5(d) and 5(e), respectively. Comparing to the NRZ, considerably better BER performance at higher received optical power can be achieved in the EDB transmission cases, in which all the spatial channels achieve BER below the KP4 FEC limit (BER = 2.0E−4).

5. Conclusions

In this paper, we experimentally demonstrated real-time 7 × 100 Gbps/λ/core IM/DD transmission over 1 km and 10 km MCF. Self-developed BiCMOS chipset and monolithic integrated DFB-EAM provide high lane rate and the in-house fabricated MCF and FI/FO modules are used to scale the lane count in spatial dimension. Over 1 km, EDB communication below KP4 FEC limit is achieved. With optical dispersion compensation, both NRZ and EDB transmission over 10 km MCF achieving 7%-OH-FEC limit are enabled. Simpler Rx configuration can be found for NRZ transmission while better transmission performance of EDB signal can be observed due to the lower bandwidth occupation. The real-time DSP-free SDM system demonstrates its potential to support high-speed DCI. Operation at 1.55 um band offers high capacity and interoperability throughout the intra-DC and inter-DC networks. In the future work, we would explore WDM technology for and further extend the current system in wavelength domain.

Funding

National Natural Science Foundation of China (61331010, 61722108, 61775137, 61671212, and 61550110240); Swedish Research Council (VR); the Swedish Foundation for Strategic Research (SSF); the Göran Gustafsson Foundation; the Swedish ICT-TNG; the Celtic-Plus sub-project SENDATE-EXTEND & SENDATE FICUS funded by Vinnova; the Flemish FWO & IWT, IOF, EU H2020 projects STREAMS (688172); TeraBoard (688510); and the Natural Science Foundation of Guangdong Province.